Korean J. Chem. Eng., **20**(1), 104-109 (2003)

Adsorption of Methane and Ethane into Single-Walled Carbon Nanotubes and Slit-Shaped Carbonaceous Pores

Byeong-Ho Kim*, Gyeong-Ho Kum* and Yang-Gon Seo†

Division of Applied Chemical Engineering/ERI, *Department of Environmental Protection,
Gyeongsang National University, 900 Gajwa-dong, Jinju 660-701, Korea
(*Received 21 June 2002 • accepted 13 November 2002*)

Abstract−The adsorption equilibria of methane, ethane and their binary mixture in single-walled carbon nanotubes (SWNTs) and slit-shaped carbonaceous pores were studied by using a Grand Canonical Monte Carlo (GCMC) method. We used a slit-shaped pore for microporous structure of activated carbons and an armchair type of cylindrical pore for SWNTs. Methane was modeled as a spherical Lennard-Jones (LJ) model and ethane as two LJ sites with the unified methyl group. The isotherms of both components in micropore region displayed Type I adsorption by Brunauer et al., which corresponds to unimolecular adsorption. At low pressure the storage capacity of SWNTs for pure components of methane and ethane was higher than that for slit-shaped pore geometries of the same size, and the selectivities of equimolar bulk gas mixture were much higher. GCMC was shown to give good qualitative agreement with Ideal Adsorbed Solution Theory (IAST).

Key words: Adsorption, Selectivity, Carbon Nanotubes, Slit-shaped Pore, Grand Canonical Monte Carlo

INTRODUCTION

Activated carbons have been the most widely used amorphous type adsorbents, and are now considered as one of the most promising gas separation systems [Patrick, 1995; Yang, 1987; Kim et al., 2001, 2002]. Because of their large internal surface and the chemically inert nature of the graphite surface they are able to adsorb non-polar and weakly polar molecules more strongly than other adsorbents. Activated carbons are produced by the graphitization of naturally occurring porous carbonaceous materials such as wood, peat, coals, coconut shells and fruit nuts, or synthetic precursors such as resins and pyrolyzing polymers. Due to the variability in the structure of the precursor materials and differences in the processing conditions, there is significant variation in the internal structure of activated carbons.

Although carbon nanotubes have only recently been discovered, they have been attracting a great deal of scientific interest due to their potential application in areas such as adsorbents and composite materials [Iijima, 1991; Lee et al., 2001]. Nanotubes have a number of graphite sheets in tube walls that can vary from 1 for single-walled nanotubes (SWNTs) to over 50 for multi-walled nanotubes (MWNTs), and inner diameter ranging from 1 nm to 5 nm with a definite diameter [Dujardin et al., 1994; Ajayan et al., 1994]. Crystallized arrays of SWNTs have a very narrow pore size distribution with virtually all their pore size in the micropore region. In contrast, pore size in activated carbon is broadly distributed between macropores, mesopores and micropores. According to the IUPAC, the pores are subdivided by diameter (D) into micropore ($D<2$ nm), mesopore ($2\ nm<D<50\ nm$), and macropore ($D>50$ nm).

†To whom correspondence should be addressed.
E-mail: ygseo@nongae.gsnu.ac.kr
‡This paper is dedicated to Dr. Youn Yong Lee on the occasion of his retirement from Korea Institute of Science and Technology.

Adsorption behavior depends strongly on the microporous structure of a particular adsorbent. The adsorption measurements reflect in an aggregate way the adsorption behavior of the individual pores. In this work the effect of pore size on the adsorption behavior is of interest. The adsorption equilibria of methane, ethane and their mixture into SWNTs and slit-shaped pores of an activated carbon were studied by using a Grand Canonical Monte Carlo (GCMC) method. We reported equilibrium isotherms of methane and ethane and selectivities for equimolar binary mixture, and showed snapshots in model pores. The simulation results in this work can be used to optimize the pore geometry for gas separation at a given pressure and temperature.

MODEL AND SIMULATION

1. The Pore Models

The pore size and shape are the most important properties in selective adsorption applications, but, in the case of activated carbon, are very difficult to define. The pore structure in activated carbon originates from the void spaces between distorted graphitic lamellae, which are highly irregular [Burchell, 1999]. In this work the

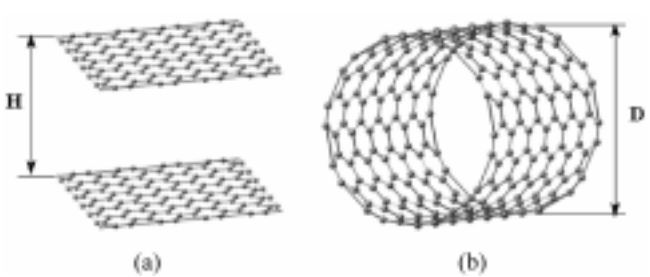

Fig. 1. Graphite sheet of slit-shaped pore in an activated carbon (a) and a segment of an armchair carbon nanotubes of diameter 1.496 nm (b).

microporous structure of activated carbon is modeled as various slit-shaped pores, which is most widely used in this field [Cranknell et al., 1994; Kaneko et al., 1994]. Fig. 1a illustrates a graphite sheet for a slit-shaped pore of activated carbon. The physical pore width, H, is defined as the distance between carbon-atom centers on these opposite walls. A standard rectangular simulation cell has been adopted to present the slit-shaped model pores with the usual periodic boundary conditions in x and y directions. The x and y dimensions of the simulation cell were set to 5.715 nm, corresponding to 15 times the molecular diameter of the methane. The adsorption in slit-shaped pores of the same diameters as SWNTs was calculated by varying the z-direction of the simulation cell.

SWNTs are found to grow in the gas phase and have been observed to cluster, forming a bundle of straws. Although the nanotubes typically have their ends capped, attempts to open the ends have met with some success [Ebbensen et al., 1994; Tsang et al., 1994]. Carbon nanotubes are cylindrical structure and consist of rolled up graphite sheet. There are two modes of rolling graphite sheet, which give rise to the armchair and saw-tooth configurations. We construct SWNTs according to the armchair mode of rolling. SWNTs constructed in this manner have only certain allowed diameters. In this work nine pore widths are considered, namely D= {0.678, 0.814, 0.950, 1.085, 1.357, 1.628, 2.032, 2.713, 3.392} nm, falling mainly into the micropore size range. SWNTs at different allowed diameters can be produced by the saw-tooth mode of rolling. Fig. 1b illustrates a segment of an armchair SWNT of diameter D=1.496 nm. D is the center-to-center distance of two diametrically opposite carbon atoms on the nanotubes walls. The boundary condition of axial direction was applied. We used a length of 7.87 nm for all simulations reported in this work. The C-C bond length of 0.142 nm corresponding to that of graphite was used.

2. Simulations

The intermolecular interactions between two molecules were given by a 12-6 Lennard-Jones (LJ) potential.

$$\phi_{ij}(r) = 4\varepsilon_{ij}\left[\left(\frac{\sigma_{ij}}{r}\right)^{12} - \left(\frac{\sigma_{ij}}{r}\right)^{6}\right] \quad (1)$$

The Steele's 10-4-3 potential [Steele, 1974] was used for interaction between a molecule and carbon pore wall in the slit-shaped pores, and the total adsorbent potential was calculated by adding contributions from both pore walls.

$$\phi_{ij}(Z) = 2\pi\varepsilon_{is}\rho_s\sigma_{is}^2\Delta\left[\frac{2}{5}\left(\frac{\sigma_{is}}{Z}\right)^{10} - \left(\frac{\sigma_{is}}{Z}\right)^{4} - \frac{\sigma_{is}^4}{3\Delta(Z+0.61\Delta)^3}\right] \quad (2)$$

$$\Phi_i(r,Z) = \sum_j \phi_{ij}(r) + \phi_{is}(Z) + \phi_{is}(H-Z) \quad (3)$$

On the other hand, fluid-wall interactions in SWNTs are assumed to follow the 12-6 LJ potential with the cut-off length. Methane was modeled as a spherical LJ model and ethane as two LJ sites with the unified methyl group. The interactions were cut at 2.286 nm which corresponding to 5 times the methane s parameter. In all of the simulations, the temperature was held constant at 298.2 K

The parameters used in this work are summarized in Table 1. The chemical potential was calculated from the temperature, pressure, and composition of the gas phase by using the Peng-Robinson equation of state, with parameters given in Table 2.

The most widely used molecular simulation method applied to adsorption problems is the GCMC simulation because it allows a direct calculation of the phase equilibrium between a gas phase and an adsorbate phase. No adjustable solid-fluid parameters were used. The implementation of this simulation method is well established [Allen and Tildesley, 1987; Frenkel and Smit, 1996]. For single component, three types of trials were used: moving a molecule, creating a molecule, and destroying a molecule.

Molecules, which are not spherical, must also be rotated. An additional trial for multicomponent systems, called a swap trial, involves switching the identity of a particular molecule and is useful for reaching the equilibrated state quickly and yielding reliable results.

Microscopic reversibility requires that the numbers of creations and destructions are equal, but there are no restrictions on the numbers of move (or swap) trials relative to the creations and destructions. However, the trials have to be performed in a random order and not follow some fixed sequence. By carrying out the trials in a random order, on average, the creations and destructions will be followed by moves (or swaps) an equal number of times. In creation trials, a new molecule is created at a random position in the pore volume, where the identity of the species is also chosen at random. However, for destruction trials, simply selecting any molecule from the simulation cell violates the criterion of microscopic reversibility. This is because the probability of destroying a particular species depends on the composition of the molecules in the pore, while in the creation trial all species are created with equal probability. Therefore, when selecting a molecule for a destruction trial, it is important to first select species at random, and then randomly pick a molecule belonging to that species.

In each step, one of these was chosen with equal probability at random. For each point on the isotherm, the system was allowed to equilibrate for 5×10^5 steps before data were collected. After equilibration, the simulation continued for 2×10^6 steps in order to calculate the average values of the extent of adsorption. Further details of the simulations are given elsewhere [Allen and Tildesley, 1984; Frenkel and Smit, 1996; Kim et al., 2001].

Table 1. Lennard-Jones parameters used in this work

	σ (nm)	ε/κ_B (K)	Bond length (nm)
Methane	0.381	148.2	
Ethane	0.351	139.8	0.235
Carbon	0.340	28.0	

Table 2. Critical constants used in the Peng-Robinson equation of state

Parameter	Methane	Ethane
Critical temperature	190.6 K	305.4 K
Critical pressure	4.60 Mpa	4.88 MPa
Accentricity factor	0.008	0.098

RESULTS AND DISCUSSION

The pure-component adsorption isotherms of methane and ethane in slit-shaped pores shown in Fig. 2 are presented as an amount adsorbed per unit volume of the pore. The basic trend observed in Fig. 2 as the pore width is increased is that Henry's constant decreases.

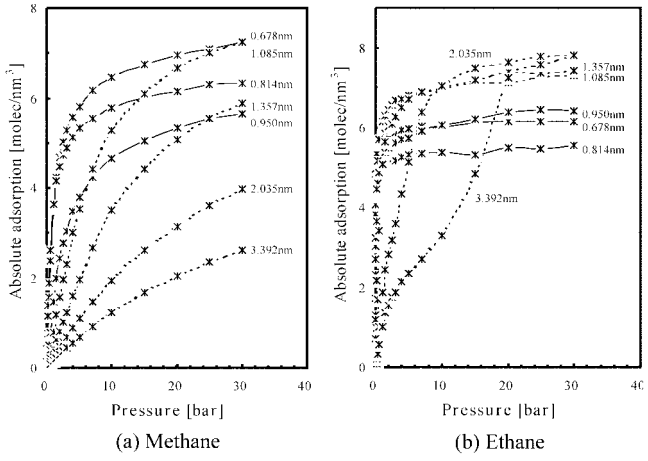

Fig. 2. Calculated adsorption isotherms for methane (a) and ethane (b) in slit-shaped model pores. Symbols are simulated points.

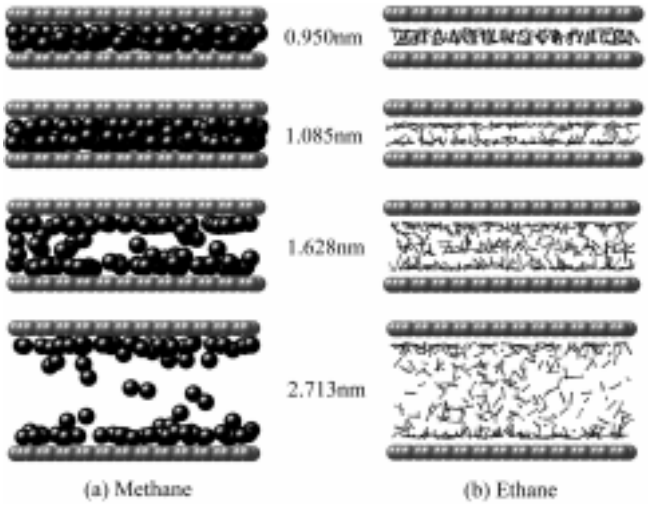

Fig. 3. Snapshots of methane (a) and ethane (b) in slit-shaped pores at P=10 bars. The gray symbols are carbon wall atoms. The solid line-segments are drawn between the individual methyl group sites in ethane. The vertical dimensions in each figure are the pore widths.

Even at low pressure the small pores fill rapidly while the large pores fill more slowly due to smaller pores having larger adsorbate-adsorbent interaction potentials. This is particularly the case for the ethane, which is more strongly adsorbed than methane. Most of the isotherms display Type I adsorption by Brunauer et al., [Brunauer et al., 1940] which corresponds to unimolecular adsorption. For some of the pore widths, the shape of the ethane isotherms is no longer Type I.

Fig. 3 shows snapshots of molecular configurations of methane and ethane in four pores of different sizes at 10 bars. The isotherms in Fig. 2 can be interpreted in conjunction with Fig. 3 which contains snapshot configurations of molecules in the same pore widths.

In the small pores the methane molecules form a very closed packing configuration due to large adsorbate-adsorbent interaction potentials. Because the small pores fill very quickly, the molecular configuration plots at 1 bar and 10 bar were very similar. As pore width increases, less closed packing configurations are displayed. The smallest pore width, which molecules of two layers form two hexagonal closed packed planes stacked one on top of the other and the potential energy is minimum, is about 1.0 nm for methane [Seo et al., 2002]. Although the molecules would adopt these precise configurations at 0 K, the packing effect is influential at higher temperatures (such as our temperature of 298.2 K). Even at higher temperatures, the hexagonal closed packing can also be formed at very high pressure. Around these pore widths adsorption of methane will reach a maximum. The adsorption will decrease as pore increases because the pore volume increases and fewer molecules in the second layer on each side are adsorbed due to weaker adsorbate-adsorbent interaction potentials.

As ethane may assume various orientations with respect to the wall, its adsorption behavior is more complicated than that of methane. At 0.950 nm ethane molecules are perpendicular to pore wall. The packing of molecules in this configuration is more efficient than molecules having to alternate between the opposing walls. Therefore, adsorption at 0.950 nm shows higher than that at 0.678 or 0.814 nm that all the molecules are aligned approximately parallel to the wall, and a complete monolayer of atoms forms (not shown in Fig. 3). At the pore width of 1.085 nm, the adsorbate splits into two monolayers, one on each surface. As pore size increases further, both the high-pressure adsorption capacity and the number of adsorbate layers increase. The larger pores, although filling more slowly, display greater adsorption at high pressures than small pores, due to the increased pore volume and ordering of the molecules. The isotherms of ethane from this pore width, i.e. 2.035 nm, begin to display Type IV adsorption because of the contribution of intermolecular attractions to the total adsorption potential and formation of multiple layers on each surface.

Fig. 4 shows the calculated isotherms of methane and ethane in SWNTs with different pore widths. Also, snapshots in SWNTs are shown in Fig. 5. Although there are some discrepancies in the absolute adsorption, the basic trends of adsorption isotherms and molecular configurations are very similar with slit-shaped pores. At 0.950 nm ethane molecules are aligned in a diametrical direction to the wall. As pore width increases, the configurations of ethane begin to rotate to tangential direction. As pore width increases further, eth-

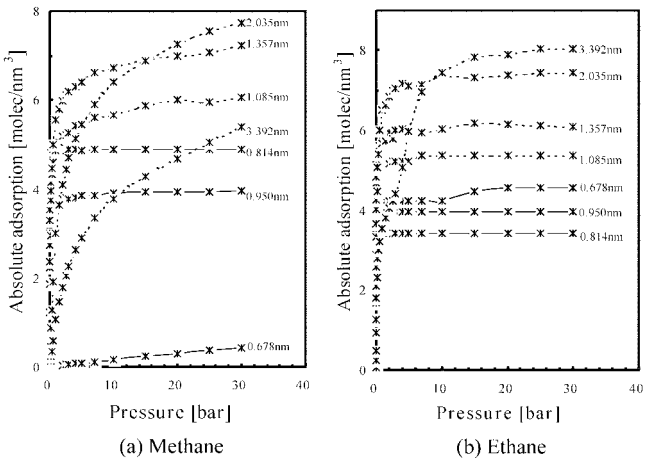

Fig. 4. Calculated adsorption isotherms for methane (a) and ethane (b) in SWNTs.

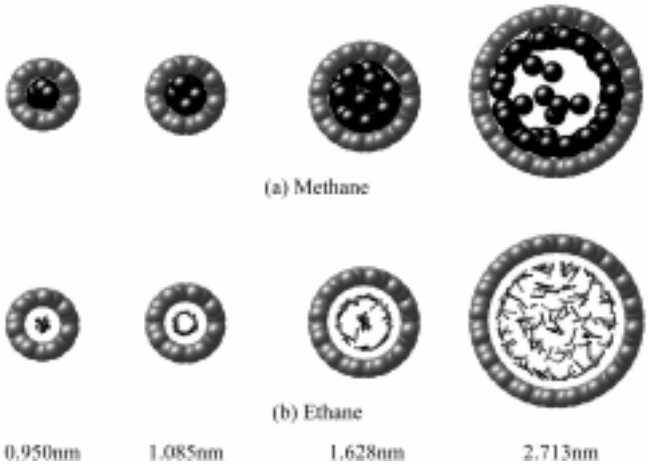

Fig. 5. Snapshots of methane (a) and ethane (b) in SWNTs at P= 10 bars. The symbols are the same as in Fig. 3.

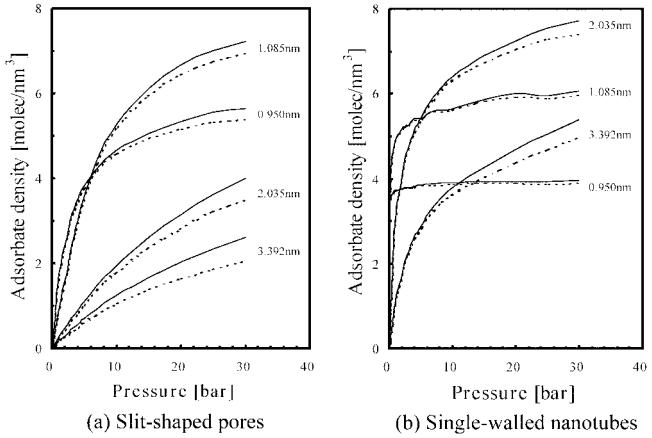

Fig. 6. Comparison of absolute and excess adsorptions of slit-shaped pores (a) and SWNTs (b). Solid lines are absolute adsorption and dashed lines are excess adsorption.

ane molecules form a second layer around the center of SWNTs by diametrical direction. At low pressure the storage capacity of SWNTs for methane and ethane is higher than that for slit-shaped pores because the adsorption potential is enhanced relative to slit-shaped pores of the same size. At higher pressure the storage capacity in micropore region is less.

Experimental adsorption measurements are presented as an excess isotherm, while the simulated adsorption generates an absolute isotherm. Therefore, before comparing simulation and experiment it is necessary to convert the simulation data to an excess adsorption isotherm. The adsorption that is calculated using molecular simulations represents the total number of molecules within the model pore. In contrast, an experimental isotherm represents the difference between the total number of the molecules within the pore and the number of molecules that would have been in the pore if no adsorption took place. The simulated isotherms are converted to excess isotherms by using a bulk equation of state to determine the number of molecules that would have been present if there were no adsorbate-adsorbent interaction.

$$N_{ex}=N_s-\rho_{bf}V_{bf} \quad (4)$$

where N_{ex} is the excess number of molecules in the simulation cell, N_s is the simulated number of molecules in the model pore size, ρ_{bf} is the bulk fluid density, and V_{bf} is the accessible volume for the bulk fluid.

This definition of the volume in which adsorption takes place has been defined in several ways [Kaneko et al., 1994; Quirke and Tennison, 1996; Gusev and O'Brien, 1997; Heuchel et al., 1999]. In this work the accessible volume for the bulk fluid is assumed to tend to zero at the smallest pore. In the case of methane, the minimum pore width that is required to determine the accessible volume for the bulk fluid using Eq. (4) was determined to be 0.61 nm for slit-shaped pores and 0.67 nm for SWNTs, respectively. The accessible volume for the adsorbate in SWNTs is less than that in slit-shaped pores because they have more carbon atoms protruding into the simulation cell. The excess adsorbate density for model pores is thus calculated by using

$$\rho_{p,i}=N_{ex}/V_{sc} \quad (5)$$

where V_{sc} is the volume of the simulation cell. The comparison of excess adsorbate density for the slit-shaped pores and SWNTs is shown in Fig. 6. At low pressure the bulk gas density is low and excess and absolute isotherms coincide. As the pressure increase, the bulk gas contribution to the total adsorption increase, until at 30 bars it represents almost 10% of the total adsorption.

The most important parameter from the point of view of mixture separation is the selectivity, S, defined by

$$S=\frac{x_1/y_1}{x_2/y_2} \quad (6)$$

where x and y refer to the adsorbed and bulk phase mole fractions, respectively.

Fig. 7 shows the binary selectivities from GCMC and Ideal Adsorbed Solution Theory (IAST) [Myers and Prausnitz, 1965] at 298.2 K with a 50% methane, 50% ethane bulk-gas mixture over a range of pressures and pore widths. The most commonly used approach to predict multicomponent adsorption is IAST based on a classical

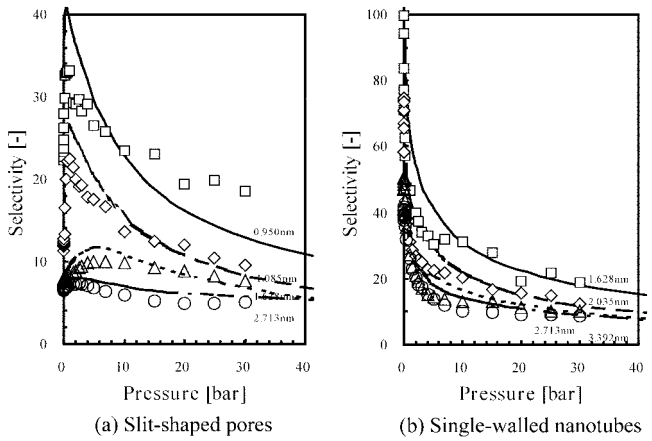

Fig. 7. Selectivity adsorption of ethane from an equimolar methane/ethane mixture. GCMC simulations (symbols) and IAST predictions (solid lines) derived from simulated single component isotherms.

thermodynamic analysis. This approach requires pure component adsorption isotherms, at the proposed temperature of operations of the adsorption unit, for all of the components in the mixture. If the bulk gas phase behaves ideally, then the standard state fugacities may be replaced by pressure, and furthermore if the individual components form an ideal gas mixture the partial fugacity coefficients are unity. The following relationship in terms of bulk pressure gives

$$Py_1 = x_1 P_1^0(\pi) \quad (6)$$

$$P(1-y_1) = (1-x_1) P_2^0(\pi) \quad (7)$$

$$\int_0^{P_1^0} \frac{n_1(t)}{t} dt = \int_0^{P_2^0} \frac{n_2(t)}{t} dt \quad (8)$$

The pure-component isotherms form the inputs to IAST, and the binary predictions, calculated from Eqs. (6) to (8), are plotted in Fig. 7. The selectivities of binary system from GCMC simulation are in good qualitative agreement with IAST. The selectivity initially increases with pressure to a maximum value and then decreases monotonically. A cooperative interaction between the ethane molecules as the pressure is increased causes an initial increase in selectivity. As pressure increases further, the adsorbate densifies and imposes an ordering of the adsorbate. The spherical methane can pack neatly into ethane molecules while the ethane is hindered molecules to rotate by confinement. This leads to decreasing selectivity. In the small pore, selectivity is a strong function of pressure and pore width, while for the pore width of 2.713 nm in slit-shaped pores, selectivity is relatively insensitive to change in the pore pressure and pore width. However, in the case of SWNTs, even up to 3.392 nm selectivities are very sensitive to pressure and pore size. Selectivities of ethane from the equimolar methane/ethane mixture in SWNTs are much higher.

CONCLUSIONS

The grand canonical Monte Carlo (GCMC) method was applied to calculate adsorption equilibria of mixture of methane and ethane. In both systems the small pores fill very rapidly, therefore displaying the largest Henry's constant. The both isotherms displayed Type I adsorption by Brunauer et al., except the case of ethane in the mesopore region. At low pressure the storage capacity of SWNTs for pure components of methane and ethane was higher than that for slit-shaped pore geometries of the same size, and the selectivities of equimolar bulk gas mixture were much higher. In the small pores selectivity from methane/ethane mixture is a strong function of pressure and pore width. In the mesopore region the selectivity was relatively insensitive to change in pressure, while in the case of SWNTs was still sensitive. The Ideal Adsorbed Solution Theory (IAST) showed good qualitative agreement with the simulation results for equimolar methane/ethane mixture. The simulation results in this work can be used to optimize the pore geometry for gas separation at a given pressure and temperature.

ACKNOWLEDGMENT

This work was supported by Korea Research Foundation Grant (KRF-2000-005-E00005).

REFERENCES

Ajayan, P. M., Stephan, C., Collix, C. and Trauth, D., "Aligned Carbon Nanotube Arrays Formed by Cutting a Polymer Resin Nanotube Composite," *Science*, **265**, 1212 (1994).

Allen, M. P. and Tildesley, D. J., "Computer Simulation of Liquids," Clarendon, Oxford, England (1987).

Brunauer, S., Deming, L. S., Deming, W. E. and Teller, E., "On a Theory of the van der Waals Adsorption of Gases," *J. Am. Chem. Soc.*, **62**, 1723 (1940).

Burchell, T. D., "Carbon Materials for Advanced Technologies," Pergamon Press, Oxford, England (1999).

Cranknell, R. F., Nicholson, D. and Quirke, N., "Grand Canonical Monte-Carlo Study of Lennard Jones Mixtures in Slit Pores; 2: Mixtures of Two Center Ethane with Methane," *Mol. Sim.*, **13**, 161 (1994).

Dujardin, E., Ebbesen, T. W., Hiura, H. and Tanigaki, K., "Capillarity and Wetting of Carbon Nanotubes," *Science*, **265**, 1850 (1994).

Ebbensen, T. W., Ajayan, P. M., Hiuri, H. and Tanigaki, K., "Purification of Nanotubes," *Nature*, **367**, 519 (1994).

Frenkel, D. and Smit, B., "Understanding Molecular Simulation from Algorithms to Applications," Academic Press, San Diego (1996).

Gusev, V. Y. and O'Brien, J. A., "Can Molecular Simulations be Used to Predict Adsorption on Activated Carbons?," *Langmuir*, **13**, 2822 (1997).

Heuchel, M., Davies, G. M., Buss, E. and Seaton, N. A., "Adsorption of Carbon Dioxide and Methane and Their Mixtures on an Activated Carbon: Simulation and Experiment," *Langmuir*, **15**, 8695 (1999).

Iijima, S., "Helical Microtubules of Graphitic Carbon," *Nature*, **354**, 56 (1991).

Lee, S. W., Park D. K., Lee, J. K., Ju, J. B. and Shon, T. W., "Discharge Capacitance of Electric Double Layer Capacitor with Electrodes Made of Carbon Nanotubes Directly Deposited on SUS304 Plates," *Korean J. Chem. Eng.*, **18**, 371 (2001).

Kaneko, K., Cracknell, R. F. and Nicholson, D., "Nitrogen Adsorption in Slit Pores at Ambient Temperatures: Comparison of Adsorption and Experiment," *Langmuir*, **10**, 4606 (1994).

Kim, D. J., Shim, W. G. and Moon, H., "Adsorption Equilibrium of Solvent Vapors on Activated Carbons," *Korean J. Chem. Eng.*, **18**, 518 (2001).

Kim, D. K., Kum, G. H. and Seo, Y. G., "Prediction of Adsorption Equilibria of Methane and Ethane onto Activated Carbon by Monte Carlo Method," *J. Korean Inst. Chem. Eng.*, **39**, 307 (2001).

Kim, S. J., Cho, S. Y. and Kim, T. Y., "Adsorption of Chlorinated Volatile Organic Compounds in a Fixed Bed of Activated Carbon," *Korean J. Chem. Eng.*, **19**, 61 (2002).

Kim, T. Y., Kim, S. J. and Cho, S. Y., "Effect of pH on Adsorption of 2,4-Dintrophenol onto an Activated Carbon," *Korean J. Chem. Eng.*, **18**, 755 (2001).

Myers, A. L. and Prausnitz, J. M., "Thermodynamics of Mixed-Gas Adsorption," *AIChE J.*, **11**, 121 (1965).

Patrick, J. W., "Porosity in Carbons," Edward Arnold, London (1995).

Quirke, N. and Tennison, S. R. R., "The Interpretation of Pore Size Distributions of Microporous Carbons," *Carbon*, **34**, 1281 (1996).

Seo, Y. G., Kum, G. H. and Seaton, N. A., "Monte Carlo Simulation of Transport Diffusion in Nanoporous Carbon Membranes," *J. Mem. Sci.*, **195**, 65 (2002).

Steele, W. A., "The Interaction of Gases with Solid Surfaces," Perga-

mon Press, Oxford, England (1974).
Tsang, S. C., Chen, Y. K., Harris, P. J. F. and Green, M. L. H., "A Simple Chemical Method of Opening and Filling Carbon Nanotubes," *Nature*, **372**, 159 (1994).
Yang, R. T., "Gas Separation by Adsorption Processes," Butterworths, Boston (1987).